Verification of LAMI vs. Synoptic Observations

Massimo Ferri and Patrizio Emiliani

Ufficio Generale per la Meteorologia (UGM), Roma, Italy

1 Introduction

The Italian version of LM, named LAMI, was included in the operational practise of UGM at the end of 2001. Verifications of LAMI forecasts are then produced on quarterly basis since the beginning of 2002. Here a synthesis of the results produced by one whole year of controls is presented.

The surface parameters analysed are 2m-Temperature, 10m-windspeed, sea level pressure and precipitation. This is due to the expectations of the users of the model, which need some indication about the constraints under which a very high resolution forecast can be used.

Furthermore the parameters under control are not explicit variables of the model but are produced through some internal post-processing which can be an extra source of error. Nevertheless, since the internal post-processing is generally based on some diagnostic balance among the model variables, which is derived from physical constraints, it is still possible to infer indication about possible problems in the formulation/configuration of the model itself.

The observations forming the control data set were collected on 3-hourly basis from the synoptic network managed by UGM. The network, including 91 manned stations, covers the entire Italian territory and is shown in Fig.1. In the following it will be given account of the results obtained in the verification of the daily cycle (temperature, wind speed and sea level pressure) and of the local precipitation.

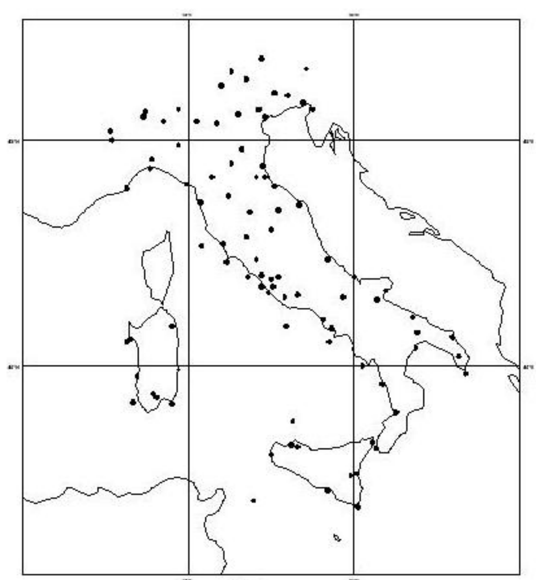

Figure 1: Synotpic network in Italy.

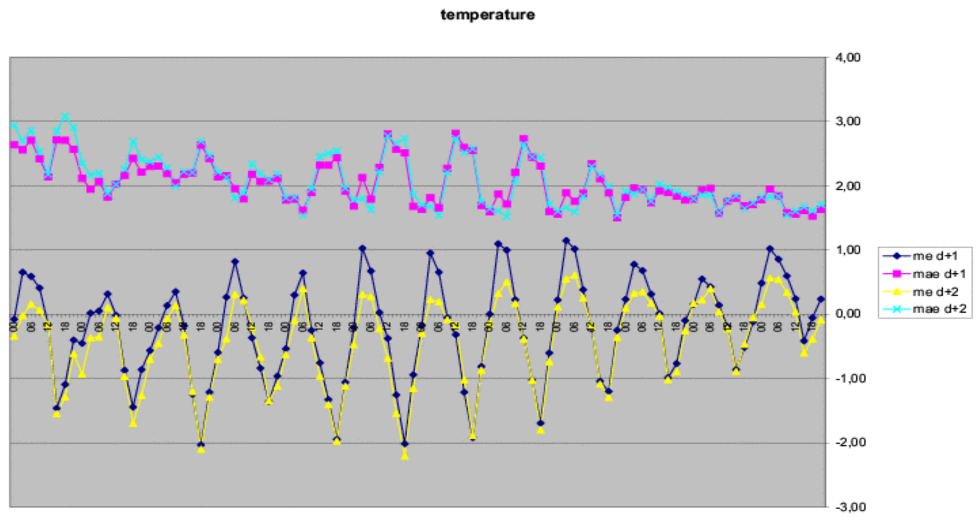

Figure 2: Mean daily cycle of temperature forecast errors for January 2002 until December 2002. Blue: mean error for day 1. Yellow: mean error for day 2. Red: mean absolute error for day 1. Light blue: mean absolute error for day 2.

2 Daily Cycle

In order to verify the diurnal behaviour of the model, the couples observation-forecast were stratified according to the hour of the day (3-hourly frequency), the month of the year and the forecast range (day 1 and day 2). Synchronous and co-located couples observation-forecast independently from the station position then form each sample. In such way systematic errors due to inconsistency in the surface representation of the model (inconsistency in the terrain elevation and in the percentage of the surface covered by water are the main error sources over Italy) are somewhat dumped and the signal of daily and seasonal oscillation is retained. For each of the 192 samples so obtained, whose size is of around 2000 elements, the mean error (ME) and mean absolute error (MAE) were computed.

Fig.2 shows the behaviour of 2m-Temperature forecast errors for day 1 and day 2. A clear diurnal oscillation is present in the ME pattern during the whole period under examination, with positive peak in the mean error around sunrise hours and more pronounced negative ones around sunset. This behaviour is present both in day 1 and day 2 forecasts but in day 1 the positive peaks are more pronounced. For what the seasonal trend is concerned, it is observed that the diurnal oscillation tend to be amplified during the summer months while the barycentre of the oscillation is well in the negative region during the warm season and closer to zero in the cold one. In the last three months the diurnal oscillations are less wide and more centred around zero.

As far as MAEs are concerned, these retain the component induced by errors in the geographical distribution of the temperature (due to the surface representation but also to the warming/cooling phases in the model forecasts). Nevertheless a clear diurnal signal is still present in the MAE curves showed in Fig.2, particularly evident in the warm season when the amplitude of the diurnal variation is of the same order of magnitude of the error amplitude. The daily variations of MAE tend to disappear in the last 3 months when the diurnal cycle of ME is dumped. Furthermore, in the last 3 months the errors are higher in the hours preceding the sunrise while in the rest of the year is the cooling after the sunset that produces greater errors.

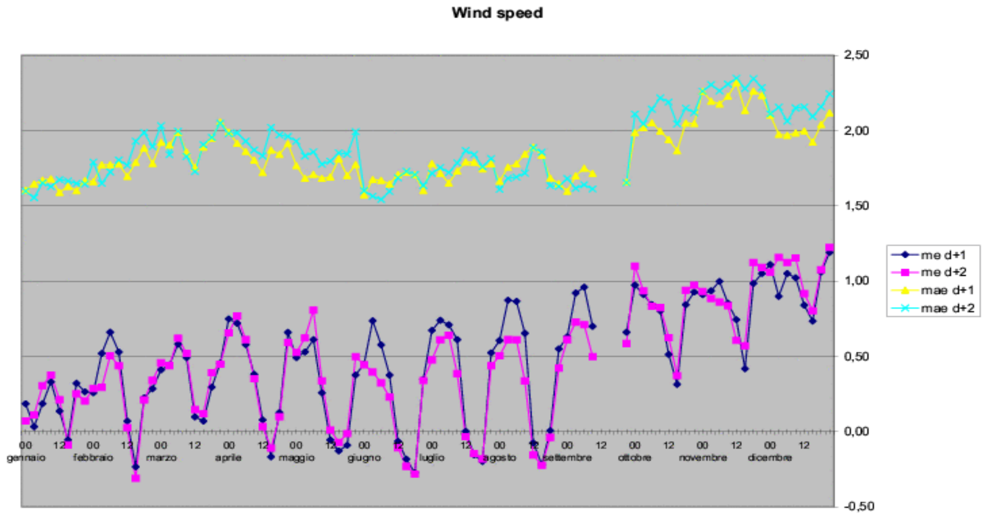

Figure 3: Mean daily cycle of 10-m wind speed for January 2002 until December 2002. Blue: mean error for day 1. Red: mean error for day 2. Yellow: mean absolute error for day 1. Light blue: mean absolute error for day 2.

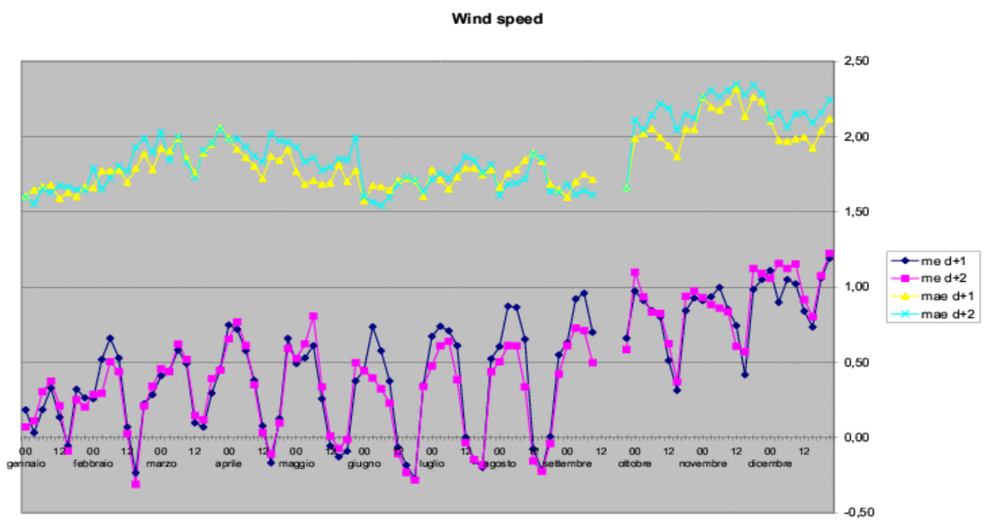

Figure 4: As in Fig. 3, but for mean sea level pressure

In conclusion verifications of 2m-Temperature along 2002 have put in evidence a diurnal error pattern well correlated with the sun phases with an excess of cooling as the sun sets and an excess of warming as the sun rises. This behaviour is more evident during the stable seasons when clear sky conditions are prevailing and is attenuated in the more active seasons (April, October, November and December) when cloudiness reduces the nocturnal cooling and the temperature distribution is driven by dynamical waves.

In Fig. 3 the curves relative to mean errors and mean absolute errors of wind speed are showed. A technical problem caused the data loss responsible of the gap in the curves for the afternoon hours of September. Even if of small amplitude (less than 1 m/s) a diurnal cycle, with maxima around sunrise and minima in the afternoon hours, is present in the ME curves. A global slight overestimation of the wind speed is attenuated in the warm stable season while is more evident during the months when dynamical circulation is dominant.

These features are present also in the MAE curves where the diurnal variations are one order of magnitude smaller than the error amplitude and the higher errors are relative to the months April, October, November and December.

The behaviour of the sea level pressure error pattern, showed in Fig. 4, is more chaotic and doesn't show any diurnal pattern regularly repeated along the year. If we compare D2 with D1, there are no signs of systematic mass loss either. Mean errors are of limited amplitude (about 0.5 hPa) while mean absolute errors are slight more than 1 hPa. The sea level pressure error pattern is less affected by local features or by the physics of the model and is dominated by the dynamics. This is evident comparing the MAEs for D2 and for D1, which are well separated during the whole year with the D2 degradation reaching its maxima during the active months (November, December).

3 Precipitation

The precipitation is the parameter for which inconsistency between the model definition (a value representing an integral over the grid cell) and the observation (a local measure) is more critical. Furthermore the intrinsic characteristic of the precipitation field (which is not continuos and highly dominated by scales not resolved by the models and in this sense can be regarded as possessing some degree of randomness) complicate even more the situation. To cope with this problem any fair comparison between the model output and the local observation should need the application of some upscaling/downscaling procedure.

On the other hand the model users tend to consider the precipitation forecasts in a crude deterministic way. This is particularly true in Italy where even the warnings issued by a public authority, such as the Civil Protection Department, are conditioned by the value of the single peaks showed by the precipitation maps produced by models.

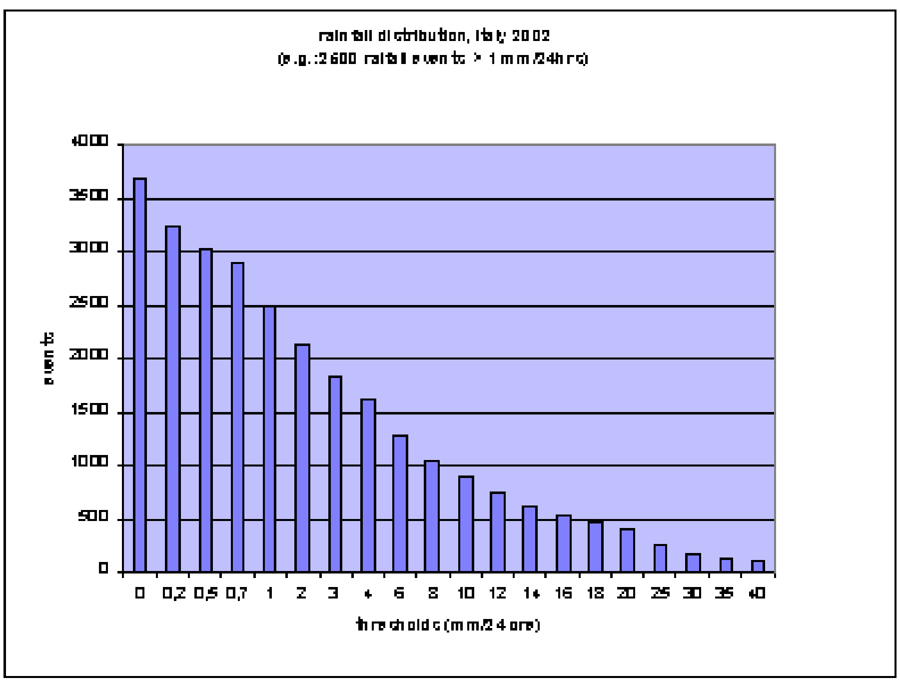

Figure 5: Frequency distribution of observed 24-h precipitation amounts for Italy: Number of cases exceeding various threshold values indicated on the x-axis.

In order to evaluate the reliability of such a deterministic approach, UGM still manages operational verification of local precipitation forecasts. Here the results of controls aimed to study the capability of the model to identify in time and space the occurrence of severe events are presented.

A data set was then built with observations coming from the network showed in Fig. 1 during the entire year, without any stratification of data. In such a way it was obtained a sample with the distribution of events showed in Fig. 5. Here the events are defined according to suitable thresholds (reported on the x-axis) and the number of cases with rainfall amount greater than the corresponding threshold was counted (reported on the y-axis). Even for the rarest event (precipitation greater than 40 mm. in 24 hours) the number of cases is sufficiently large (more than 100 cases) to consider the results obtained statistically stable.

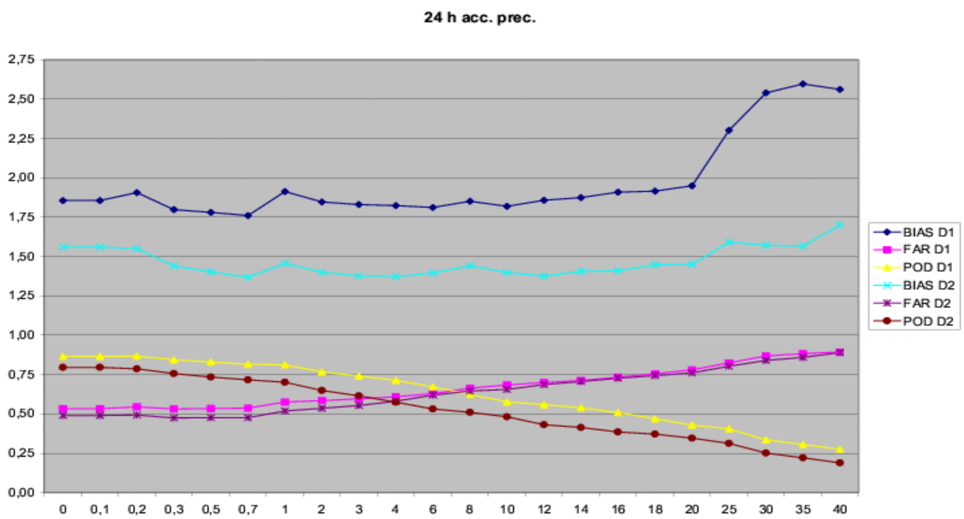

Figure 6: Frequency Bias (BIAS), Probability of Detection (POD) and False Alarm Rate (FAR) for 24 hour accumulated precipitation forecasted for day 1 (D1) and day 2 (D2) – see legend – for various thresholds indicated on the x-axis.

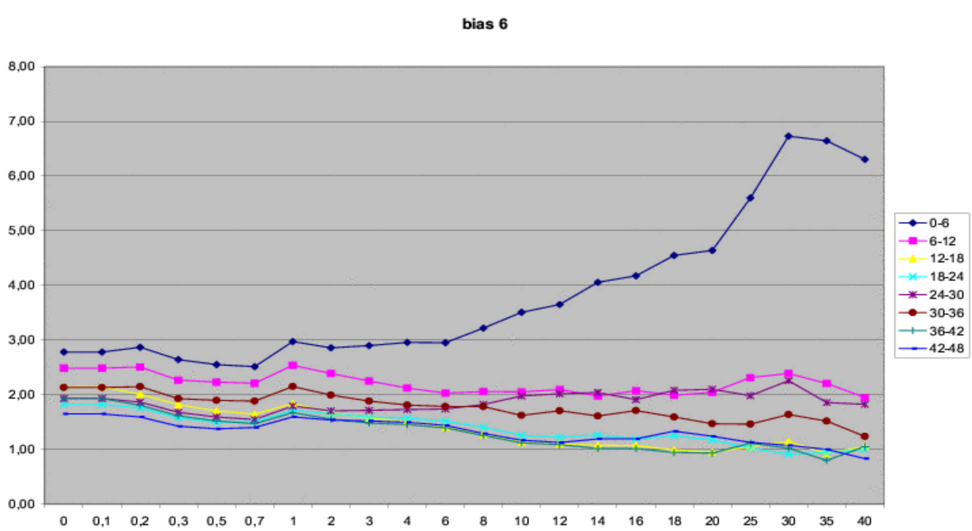

Figure 7: Frequency bias of 6-h accumulated precipitation for various thresholds indicated on the x-axis and for various forecast ranges – see legend.

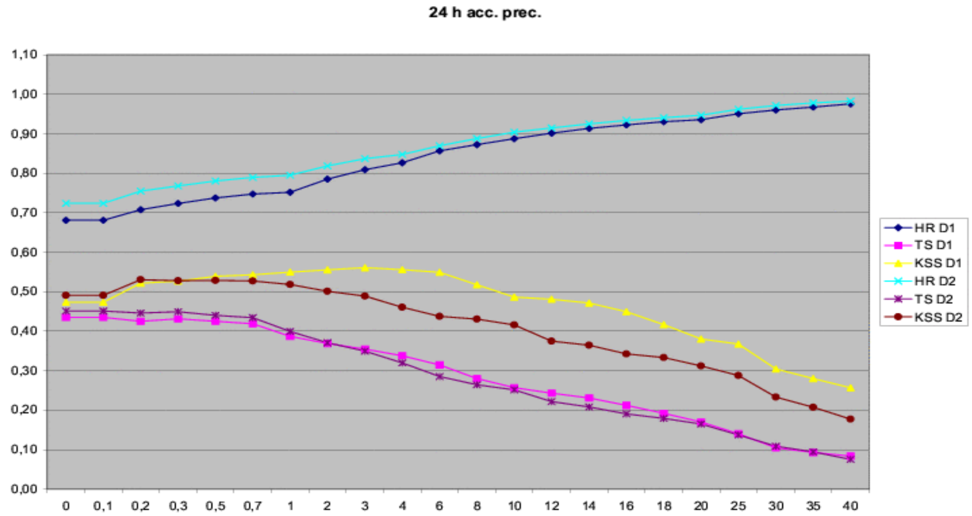

Figure 8: Hit Rate (HR), Threat Score (TS) and Kuiper Skill Score (KSS) for 24 hour accumulated precipitation forecasted for day 1 (D1) and day 2 (D2) – see legend – for various thresholds indicated on the x-axis.

In Fig. 6 Frequency Bias, Probability of Detection and False Alarm Rate for 24 hour accumulated precipitation forecasted at D1 and D2 are showed. The difference in Frequency Bias between D1 and D2 is effect of a spin up problem probably originated by the interpolation from the global fields of GME (LAMI is operationally started from interpolated analysis). This is confirmed by Fig. 7, where 6 h precipitation are considered along the two forecasted days, which shows a clear departure of the first 6 hours interval from the rest of the forecast.

Apart from this spin up problem, the flat pattern of D2 Frequency Bias testifies of the capability of the model to produce a distribution of events similar to reality but with a systematic 50matching point between POD and FAR curves is assumed as criterion to assess the usefulness of the forecast, we see that the thresholds that can be used to distinguish local events are no more than 6mm/24h for D1 and 4mm/24h for D2.

On Fig. 8 analogous curves for Hit Rate, Threat Score and Kuiper Skill Score are reported. If we assume 30condition for Threat Score, usable thresholds are again 6 mm/24h for D1 and 4 mm/24h for D2.

In conclusion the use of LAMI direct output, and in the opinion of the writers of any high-resolution model, to localise in time and space the occurrence of severe events is subjected to strict limitation. Some de-localisation procedure, conserving the realistic distribution of events showed by the model, is needed in order to get a better operational exploitation of the high-resolution precipitation field produced by the model.